

JAN ŚRODOŃ¹

AN INTERPRETATION OF CLIMBING-RIPPLE CROSS-LAMINATION

(Pl. I—II and 5 Figs.)

Interpretacja ryplemarków wstępujących

(Tabl. I—II i 5 fig.)

Abstract. The development of climbing-ripple cross-lamination has been studied theoretically, on the basis of the sediment transport theory of R. A. Bagnold. The following new factors controlling the pattern of current climbing ripples were recognized: 1) the bulked sediment size changes, 2) the limited availability of transportable solids, and 3) the maturation of the rippled bed pattern. There are three main measurable quantities constituting each pattern: 1) the angle of climb of the ripples, 2) the bulked sediment size, and 3) the ripple height. Allen's (1973 b) classification of climbing-ripples is expanded and slightly modified. The outline of the genetic interpretation of these structures is suggested.

HYDRAULIC CONDITIONS OF CLIMBING-RIPPLE STRUCTURE DEVELOPMENT

The climbing-ripple cross-lamination (climbing-ripple, ripple-drift cross-lamination, ripple-drift, climbing small-scale cross-stratification) is a somewhat ambiguous term as used in the present geological literature. Traditionally, the term has been applied to „cross-stratified deposits in which can be seen a definite ripple topography associated with the climbing of one ripple up the stoss side of the ripple immediately downstream” (Jopling and Walker, 1968, p. 972). Recently, Allen (1973 a) refers to every internal structure, in which the angle of climb of the cross-laminated units exceeds, on average, zero degree relative to the generalized bedding surface, as climbing-ripple. In the present paper, the traditional, very restricted sense of the term is accepted. Consequently,

¹ Pracownia Sedymentologii ZNG PAN, 31-002 Kraków, Senacka 3.

climbing-ripple cross-lamination is regarded as a particular regular variety of small-scale cross-lamination. Climbing-ripple structure results from the sedimentation of grains on the active rippled bed. Such a genetic interpretation of climbing ripples was already given by Sorby (1908) and confirmed experimentally by McKee (1965), Allen (1971 b) and Southard et al. (1972). McKee (1965) pointed out that the climbing-ripple structures may result from the wave as well as the current action. The present study deals with the latter case exclusively. The conditions of the formation of the current climbing ripples may be listed as follows:

- 1) A combination of fluid flow and transported sediment parameters resulting in the formation and stability of the ripple-type bed.
- 2) The type of flow during which the deposition can take place.
- 3) The average life-time of ripples relatively long, as compared with the time, during which the coset is formed.

The third requirement is distinctive for climbing ripples, while (1) and (2) apply to any kind of small-scale cross-lamination. For the sake of clarity, the fore-said requirements should be discussed separately.

1) Gilbert (1914) was the first to distinguish experimentally four bed regimes, considering the increasing flow strength: plane bed, dunes (= ripples), plane bed, antidunes. However, the most stimulating approach to the rippled bed problem was presented by Bagnold (1956, 1966). Bagnold regarded ripples as a form of bed roughness which exerts a form drag, necessary to offset the deficit of bed resistance to fluid shear stress, when bedload transport takes place, although is not fully developed. The field of the rippled bed stability, as understood in the present article, is — approximately — coincident with the range of the bedload transport development: $\Theta_1 < \Theta < \Theta_2$ (fig. 1), where Θ is a dimensionless quantity, expressing the relation between the parameters of fluid flow and transported sediment:

$$\Theta = \frac{\tau}{(d_g - d_f) g D} \quad (1)$$

in which τ is the fluid shear stress, d_g and d_f — the grain and fluid density respectively, g — the acceleration due to gravity, and D — the grain diameter. Θ_1 is the threshold of bed movement, and Θ_2 — the threshold of fully developed bedload transport.

The data presented by Bagnold (1966) (fig. 1) suggest that ripples could not form when the grain size is less than approximately 0.02 mm ($\Theta_1 \cong \Theta_2$). However, Rees (1966), in his flume experiments with 10 μ m clay-size free silt, pointed out that, in the presence of excess material in suspension, ripples are stable within $\Theta = 0.1$ — 0.4 range (fig. 1). In the absence of the excess material, the plane bed appeared to be stable over the entire range. Rees postulated dual values of Θ_1 to explain that phenomenon.

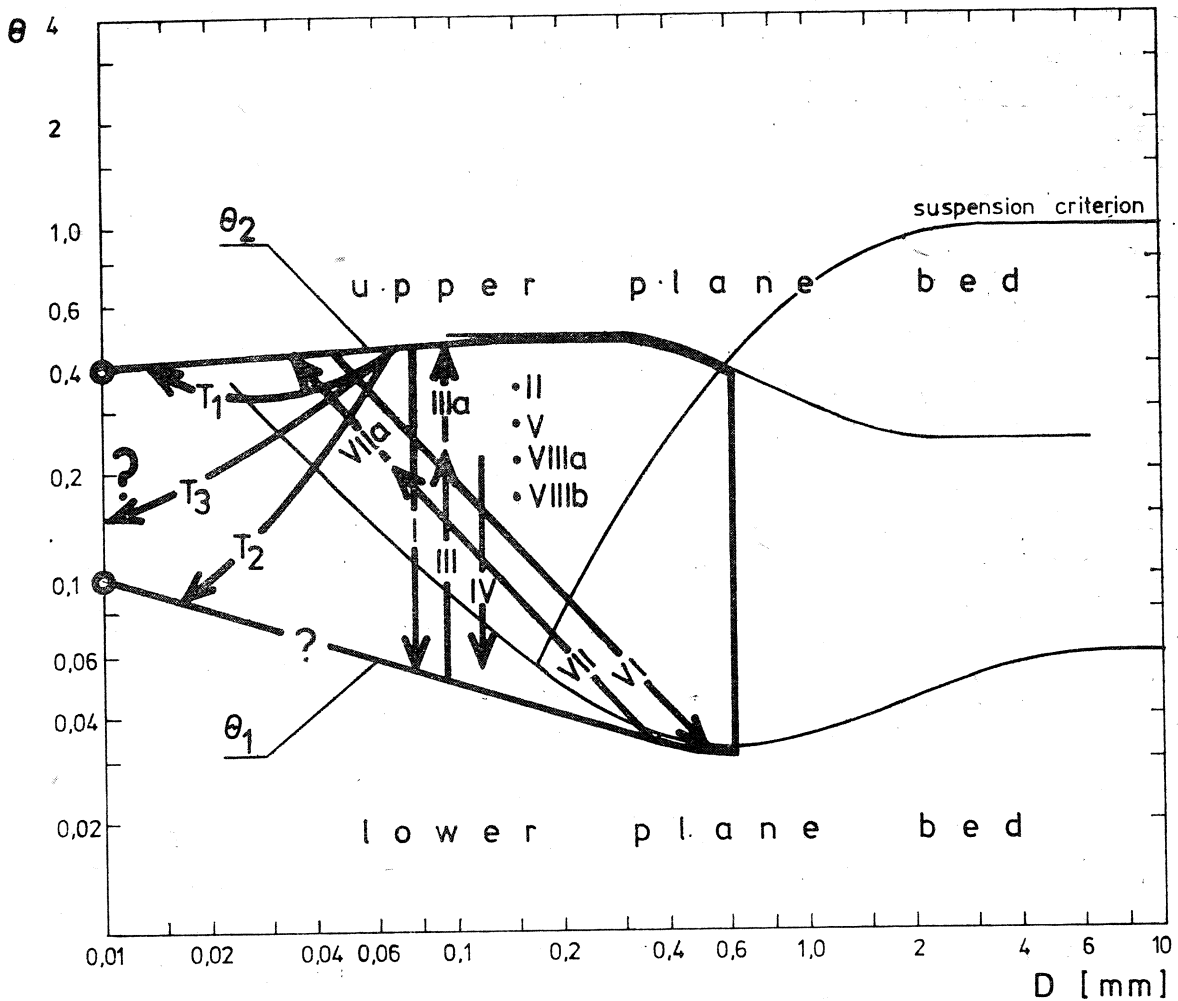


Fig. 1. The flow stage diagram with stability field for the rippled bed, assuming the presence of excess material in suspension [after Bagnold's data (1966, fig. 4 and 8) — thin lines, modified and completed in the fine grain end according to Rees (1966) — open circles]. The simple climbing-ripple patterns, listed in fig. 5, are indicated here by arrows or points, marked with Roman numbers. The T_1 , T_2 , T_3 arrows represent the three main theoretical complex patterns for turbidites

Fig. 1. Pole trwałości ripplemarków w sytuacji obecności materiału w zawiesinie [wg danych Bagnolda (1966) — cienkie linie, uzupełnionych w zakresie frakcji pyłowej na podstawie danych Reesa (1966) — kółka]. Strzałki i punkty oznaczone cyframi rzymskimi symbolizują proste wzory ripplemarków wstępujących, zestawione na fig. 5. Strzałki oznaczone symbolami T_1 , T_2 , T_3 reprezentują trzy główne wzory złożone występujące w turbiditach

The Rees's experiments suggest that the lower grain size limit of ripple formation is determined exclusively by the cohesion of the sediment. According to his opinion (1966, p. 237), „it is probable that the cohesion commonly observed in fine sediments is due to the presence of a fraction of clay-size material”. Thus, the ripple stability field, as based on Bagnold's research (1966) and modified — using Rees's (1966) data (fig. 1) — should be assumed as generally valid on the left of the diagram, provided D is regarded exclusively as a grain size of a very narrow class, and not as the median or the arithmetic mean of the grain size of a heterogeneous material. The precise evaluation of the lower

grain size limit and an extremely fine grain size distribution of ripple-forming material needs further experimental studies.

The upper grain size limit of ripple formation, about 0.7 mm, has been established theoretically by Bagnold (1966) and confirmed experimentally (Simons et al., 1965; Southard and Boguchwal, 1972).

2) The predomination of deposition over erosion is an apparent condition for any internal structure to be preserved. The climbing-ripple structure reflects an uninterrupted deposition throughout the formation of the entire coset. The deposition takes place when the sediment transport rate declines with time, downcurrent or both with time and downcurrent (i.e. in case of the decaying unsteady, decaying non-uniform and unsteady non-uniform flow). In the mathematical sense these cases correspond to the negative value of the deposition rate ($M < 0$), as the latter is a derivative of the sediment transport rate with respect to distance, time or both of them (Allen, 1970, 1971 b). These distinctions are only valid in case of an unlimited availability of transportable solids. The significance of this condition, which has not been previously discussed by Allen, will be demonstrated below.

3) The regularity of climbing ripples, as observed usually in the vertical cross-sections parallel to the flow, implies two further conditions:

1. The rippled bed pattern should be rather time-stable, especially if the deposition rate is not very high. Allen (1973 a), in his interesting experimental work, has shown that the fluctuating component of the ripple migration velocity, controlling the stability of the rippled bed pattern is proportional to the ripple velocity itself. The latter grows with the mean fluid flow velocity. On the other hand, it must be remembered that the increasing deposition rate and the increasing time-stability of rippled bed pattern effect the regularity of climbing ripples in the same way.

It has been suggested earlier that high deposition rates are connected with a well developed suspended load transport (Sanders, 1963; Jopling and Walker, 1968). Referring to fig. 1, we can predict that the domination of the suspended load transport can take place if the majority of the grains in the transported material have the threshold of suspension (suspension criterion) lower than the threshold of bedload movement ($D < 0.2$ mm for clear water).

The factors discussed above point out relatively slow but quickly decaying currents overloaded with medium or fine sands or silts, as the most suitable environment for the formation of climbing ripples. The textural characteristics of the published instances support the above conclusion (Sorby, 1908; McKee, 1938, 1966; Wood and Smith, 1958; Walker, 1963; Coleman and Gagliano, 1965; Davies, 1966; Boersma, 1967; Kuenen, 1967; McKee et al., 1967; Jopling and Walker, 1968; Aario, 1972).

2. It seems obvious that the geometry of the ripple pattern on the bottom also effects the regularity of the climbing-ripple pattern. As a rule, more or less two-dimensional forms, in preference to the three dimensional ones, following Allen's classification (1968), should favour the formation of more regular internal structures. For instance, the ripples shown on Pl. I, fig. 1, correspond to the climbing-ripple pattern presented on Pl. I, fig. 2. The extensive research by Aario (1972) supports the above idea, though he also has provided illustration for an interesting exception (Pl. 4, fig. 4).

In natural associations of bed forms, two-dimensional ripples usually succeed three-dimensional ones with increasing depth and decreasing current velocity (vide Allen, 1968 p. 93). This tendency supports the earlier conclusion, as far as the conditions favouring the formation of climbing ripples are concerned.

THEORETICAL EVALUATION OF CLIMBING-RIPPLE PATTERNS

Discussion of results of Allen's research

According to the two-tier classification of climbing ripples, proposed by Allen (1973 b), „pattern” denotes some type of the vertical changes of the angle of climb and the bulked grain size, distinguished at the level of the coset. The three patterns defined by the author (Allen, 1973 b) have been deduced by him earlier (Allen, 1970) from the relation:

$$\tan \zeta = \frac{MH}{2 j_b} \quad (2)$$

in which ζ is the angle of climb of the ripples, M is the rate of sediment transfer in a direction normal to the generalized bed, the rate being negative in the case of deposition, H is the ripple height, and j_b is the bedload transport rate.

Following Allen's analysis, we find that, at any fixed point, $\tan \zeta$ is controlled by the deposition rate M , the mean fluid flow velocity \bar{U} , the ripple height H , the grain size of transported material D , the densities of transported sediment d_g and transporting fluid d_f , the fluid viscosity, and the flow depth (the latter two contained implicitly in bed shear stress τ). Allen investigated analytically (1970) the influence of the two most important parameters M and \bar{U} on $\tan \zeta$, putting all the others as constants. In a further research (1971 b), he expressed the mean grain size D as a function of \bar{U} and modified slightly his earlier equation (2). For the requirement of the present study, the simpler, approximate equation (2) is considered to be quite sufficient. Allen's results in the genetic interpretation of climbing ripples variability at a single vertical profile may be summarized briefly as follows (see also fig. 5):

1. If the mean flow velocity \bar{U} declines downcurrent (non-uniform flow), $\tan \zeta = \text{const.}$ at any fixed point. The mean size of bulked sediment should also be constant. It is the case of Allen's (1973 b) pattern II. On the flow stage diagram (fig. 1), that pattern is represented by any point within the field of ripples stability.

2. If \bar{U} declines with time (unsteady decaying flow) and, eventually, some variation of \bar{U} downcurrent takes place as well (unsteady decaying non-uniform decaying or accelerating flow), the most common result is the vertical upward steepening of the angle of climb (pattern I). In the case of heterogenous sediment supply, the parallel decrease in the mean grain size of the bulked sediment should be observed. On the ripple stability field (fig. 1), that pattern may be expressed by the arrow perpendicular to the ordinate (D changes are not essential to constitute the pattern) and pointing from Θ_2 to Θ_1 .

3. If the unsteady accelerating non-uniform decaying flow does not erode, it results in a vertically upward monotonic decrease in the angle of climb, accompanied by a parallel increase in the mean size of the bulked sediment (pattern III). The graphic representation of the case is the arrow perpendicular to the ordinate and pointing upward.

4. In one of Allen's papers (1971 b, fig. 5), we find a suggestion that a fourth pattern may also exist: a simultaneous decrease in the angle of climb and the mean grain size due to the deposition from the non-uniform unsteady current, accelerating and decaying respectively. That case has been marked on fig. 1 by the arrow parallel to that from p. 3 but pointing in the opposite direction.

It should be emphasized that in the deductions of Allen the mean grain size is a function of the mean flow velocity and not an independent quantity.

Despite the fact that Allen's theory is all right formally and confirmed experimentally (Allen, 1971 b), it is evident that any deductions in the opposite direction, i.e. from a pattern to a flow type, are not justified. The influence of other variables on the $\tan \zeta$ should be checked earlier. According to the author's experience, only the changes of D and H can be geologically significant. The third situation to be considered is that of the basal condition not being fulfilled, i.e. when availability of transportable solids is limited. Below, we shall deal with these three problems.

Changes of the ripple height

According to the eq. 2, the ripple height H is one of the factors controlling the value of the $\tan \zeta$. The most important deposition conditions, involving H changes, may be listed as follows:

1. sediment size changes (Inman, 1958; fide McKee, 1965; McKee, 1965).

2. mean flow velocity or wave strength changes (Bucher, 1919 and Evans, 1942; both vide McKee, 1965; McKee 1965; Rees, 1966; Scheidegger and Potter, 1967; Allen, 1973 a).

3. maturation of the rippled bed pattern (McKee, 1965; Rees, 1966).

4. transition from the rippled bed to the upper plane bed.

No. 1 case will be discussed in the next chapter, as the grain size changes themselves appear to be the dominating factor.

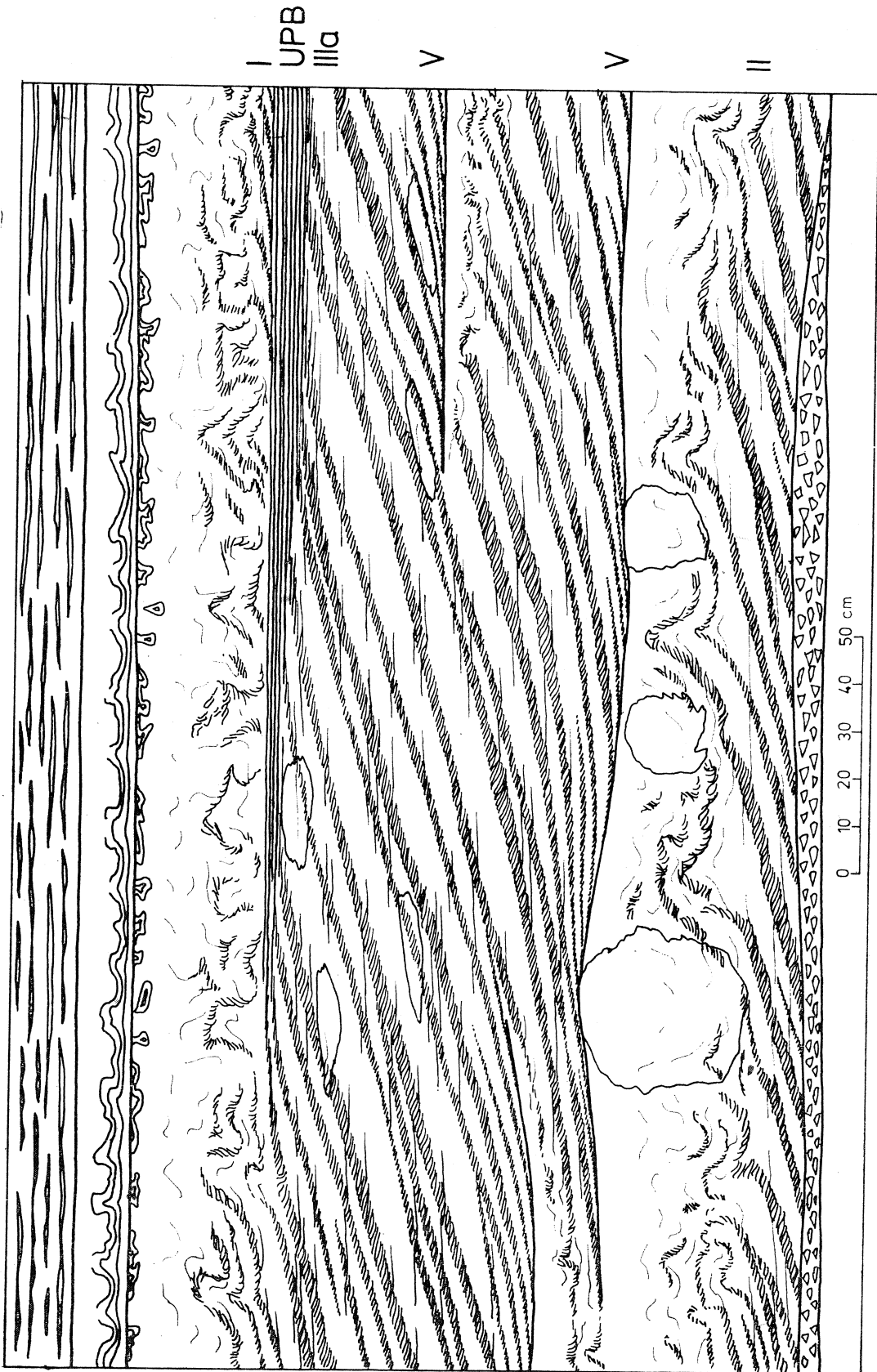
According to the evidence of the experimental works quoted, the ripple height increases or decreases as the mean flow velocity increases or decreases respectively. It implies that the H and \bar{U} changes will have opposite effects on $\tan \zeta$ (pattern I and III) or the effects will be summed up (pattern IV). The changes of H , as compared with those of M and j_b (eq. 2, fig. 5) are very limited, or even undetectable in some experimental conditions (Allen, 1971 b). Hence the analysis developed by Allen (1970, 1971 b) remains valid. Probably, the H changes can usually only slightly modify the patterns due to the fluid flow changes.

An exceptional case is that of the climbing ripples building up at the stage of flow close to the upper limit of the ripples stability field (Θ_2 — fig. 1). A further acceleration of the current will result in a transition to the upper plane bed conditions. The produced pattern is geometrically and texturally quite similar (fig. 5) to Allen's pattern III, but its genesis is different. The dominant quantity controlling the angle of climb decrease down to zero degree is the decreasing ripple height $H \rightarrow 0$. The

diminishing ratio $\frac{M}{j_b}$ supports that trend but its influence may be either significant or rather slight. The pattern considered presently is represented on the graph (fig. 1, IIIa) by the upward arrow, perpendicular to the ordinate and touching the Θ_2 line.

The most characteristic feature for identifying the pattern described is the flattening of ripples in the upper part. The continuous vertical upward transition into horizontal lamination (upper plane bed) should be observed normally if the deposition rate remains negative over the transition region.

There is widespread field evidence to show that the transition from the upper plane bed to the rippled bed — and not from upper plane bed to dunes, and subsequently to ripples, as the flume experiments would suggest (Simons et al., 1965) — is frequently reflected in the climbing-ripple structure (Sorby, 1908; Bouma, 1962; Ballance, 1964; McKee et al., 1967; Allen, 1971 a, b; Blatt et al., 1972, fig. 5—10). The alternative transition from climbing ripples to horizontal lamination is far less common. The two examples I have found in literature are those of Coleman and Gagliano (1965, fig. 5) and Aario (1972, fig. 18). Unfortunately, the transition zone is disturbed by convolute deformation in the former instance, and the other sketch is very schematic.



Some good examples of the pattern which reflects the transition from the rippled to the upper plane bed have been observed by the author in the Carboniferous montmorillonitic claystones from the Upper Silesian Coal Basin. Unfortunately, I have failed to get a good photograph and subsequently the profile has been destroyed by exploitation. Thus, my hand drawing (fig. 2) is the only record preserved. The horizontally laminated layer UPB ascribed to the upper plane bed shows — as compared with the climbing ripples under- and overlying it (IIIa and I) — a considerable increase in coarser grades (fig. 3).

The rôle of the vertical upward transition to the upper plane bed in constituting some patterns characteristic for turbidites will be discussed in the next chapter.

The opposite situation to the decay of ripples is that of the ripples appearing and maturing on a plane bed. It is a unique process which can make the angle of climb steepen up the profile in the stabilized conditions of fluid flow and sediment supply (non-uniform flow). $\tan \zeta$ increases parallel to H , as $\frac{M}{j_b}$ remains constant (eq. 2).

The process considered presently involves a growth of the ripple height and the length accompanied by the reduction of the number of ripples per length unit parallel to the flow, some of the ripples being captured by some other ones. The experimental process of maturation has been illustrated particularly well by Rees (1966). In his experiments with 10 μm silt, the maturation continued during a period longer than 24 hrs.

The geological conditions necessary for the above described structure to appear should be rather uncommon. They include the destruction of the ripples formed in non-uniform current without any change of the flow conditions and they also include a succeeding reconstruction of the ripple pattern on the flat bed. The unique record of the considered process

Fig. 2. A vertical cross-section of the climbing-ripple coset in Carboniferous montmorillonitic claystones, broadly speaking, parallel to the flow direction (flow from left to right). Pattern II due to non-uniform flow dominates throughout the coset. Pattern V, ascribed to the maturation of the rippled bed pattern, overlies the smooth planes formed locally by liquefaction (lower part). In the upper part, a transition (pattern IIIa) to the upper plane bed (UPB) and back to the rippled bed (pattern I), the latter strongly disturbed by convolute deformation. The concretions are composed of the veinlets of fibrous calcite

Fig. 2. Warstwa ripplemarków wstępujących z iłowców montmorillonitowych z GZW, widziana w przekroju pionowym, mniej więcej równoległym do kierunku prądu (przepływ z lewa na prawo). W całej warstwie dominuje wzór II. Wzór V, związany z dojrzewaniem powierzchni ripplemarkowej pojawia się nad płaskimi stropami upłynnionych części warstwy. W górnej części rysunku widoczne jest przejście (wzór IIIa) ripplemarków w laminację poziomą (UPB), związaną z fazą górnego płaskiego dna. Wyżej pojawiają się znowu ripplemarki wstępujące (wzór I), zaburzone przez deformacje konwolutive. Wszystkie konkretje zbudowane są z żyłek włóknistego kalcytu

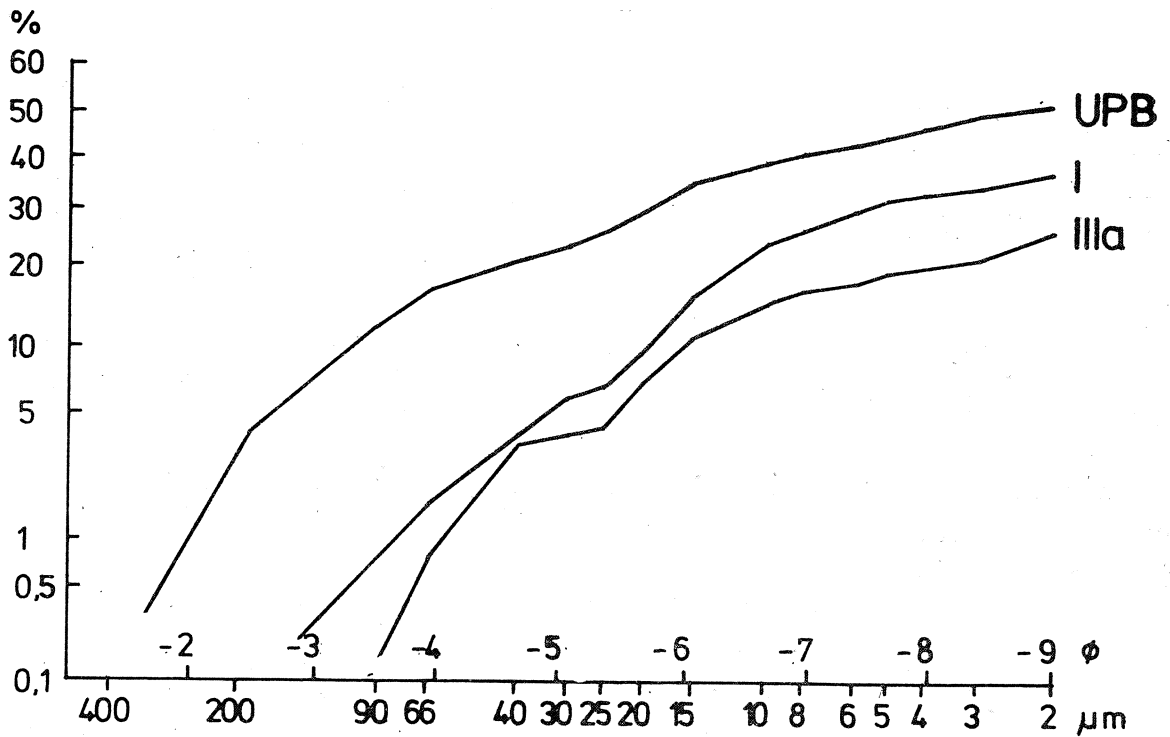


Fig. 3. The cumulative size frequency curves of bulked material from IIIa, UPB and I layers shown in fig. 2 (the measurements by the sedimentation-balance method). An apparent increase of coarse grades in UPB layer ascribed to the upper plane bed sedimentation

Fig. 3. Analizy uziarnienia warstw IIIa, UPB i I (por. fig. 2) wykonane przy pomocy wagi sedymentacyjnej. Zaznacza się wyraźny wzrost uziarnienia w warstwie UPB, interpretowanej jako osad fazy górnego płaskiego dna

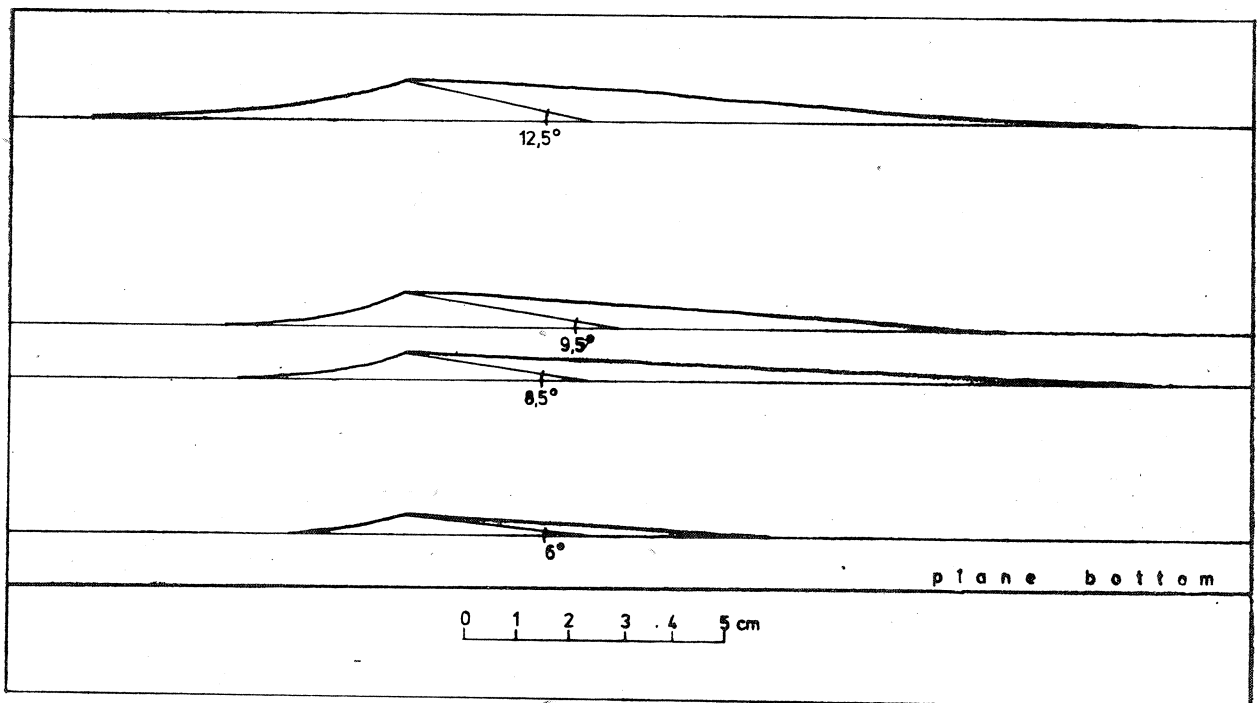


Fig. 4. Vertical changes of the shape, the dimensions, and the angle of climb of the ripples, due to the maturation of the rippled bed pattern (measurements from the sample presented on Pl. II, fig. 4)

Fig. 4. Pionowa zmienność kształtu, wielkości i kąta wspinania się ripplemarków w procesie dojrzewania powierzchni ripplemarkowej (wg pomiarów okazu widocznego na Pl. II, fig. 4)

has been shown on Pl. II, fig. 3 and 4 as well as in fig. 2 and 4. The flow conditions can be regarded as generally non-uniform throughout the coset 1—2 m thick, except for the uppermost layer (fig. 2). Locally, some bed areas have been smoothed by liquefaction and then the trains of ripples were rebuilt there (fig. 2, Pl. II, fig. 3). In the investigated profiles over the area approx. 1 km² the phenomenon was repeated 2—12 times. In the layer about 20 cm thick above the liquefaction plane, the angle of climb of the ripples increases from 0° to about 20°, i.e. the average for the entire area. The changes of the angle of climb and of the ripple dimensions during the maturation are shown in fig. 4. The rock containing these structures is now the montmorillonitic claystone (the median grain size $D_m \cong 2 \mu\text{m}$), with coal detritus and mica concentrated in the lees. The material deposited was probably volcanic glass silt ($D_m = 10\text{—}30 \mu\text{m}$) (J. Šrodón, in preparation).

It should be emphasized that the maturation process in fine grained sediments may last relatively long (Rees, 1966). Consequently, some visible traces of the process are likely to be detected in the bottom parts of any cosets starting from a plane surface. The ripple height increase and the capturing process are the two characteristic phenomena. In the most common case involving the decaying unsteady component of the current velocity, the maturation supports the flow velocity in steepening the angle of climb of the ripples. I should say it is the right interpretation of the bottom parts of the patterns shown on Pl. I, fig. 2 of the present paper, in fig. 6 of Kuenen (1967), and in fig. 116 of Picard and High (1973).

Changes of the bulked sediment size

As pointed out earlier, ripples can be formed from the material of a narrow grain class D in a broad range of the flow velocities limited by Θ_1 and Θ_2 . In the natural conditions, the transported solids are usually heterogeneous in size. It is widely known that, as a rule, simultaneously to the flow decay or acceleration, the grain size of transported material also decreases or increases respectively. The physical explanation of this phenomenon has been given by Bagnold (1966). That is why Allen (1973 b) anticipates — as a rule — an upward monotonic decrease and increase of the bulked sediment size for his pattern I and III respectively. However, the functional relation between the mean flow velocity and the sediment grain size, though very common, is not the sole situation detectable in the natural environment. Thus, let us consider how the grain size, regarded as an independent quantity, could effect the climbing-ripple patterns. For the sake of the simplicity of the analysis, we shall start with the case of the non-uniform current. The changes in the grain size spectrum of the transported sediment at a given cross-section of

non-uniform flow are theoretically possible as an effect of the changes in the source area. Replacing τ in eq. 1 with Darcy-Weisbach function for open channels, we arrive to:

$$\Theta = \frac{f \, d_f \, \bar{U}^2}{8 (d_g - d_f) \, gD} \quad (3)$$

where f is the Darcy-Weisbach coefficient of friction. The outcome of the analysis of eq. 3 is that the change of deposition conditions $\Theta_1 \longleftrightarrow \Theta_2$ may result from an adequate change of \bar{U} as well as D . When the grain size keeps growing and $\bar{U} = \text{const.}$, the hydraulic conditions resemble those of Allen's pattern I (fig. 5) because $j_b \rightarrow 0$ and $M \rightarrow \text{const.} > 0$, the value of M at Θ_1 being determined by the rate of deposition from suspension exclusively. Of course, the grain class $D < 0.2$ mm must be present (fig. 1). As a result of a considerable grain size increase in non-uniform flow we should therefore expect a steepening of the angle of climb and sinusoidal ripple lamination (sedimentation from suspension), succeeding the climbing ripples.

In the case of decreasing grain size, the hydraulic conditions may become analogical to those of Allen's pattern III or pattern IIIa, the latter presented in the foregoing chapter (the transition between the rippled bed and the upper plane bed). The latter pattern results from the ripple height decrease down to zero degree. It is well worth remembering that in the two former cases out of the three discussed above, H changes due to the varying D effect $\tan \zeta$ in the same direction as the dominating quantity (j_b). The conclusion presented is based on the fact that — according to the results of the experimental work by Inman (1958, vide McKee 1965) confirmed by McKee (1965) — the ripple height is related directly to the sediment grain size.

Referring to eq. 3, we find that the function $\Theta = f(D)$, provided $\bar{U} = \text{const.}$, may be roughly ($f = \text{const.}$) regarded as a hyperbole:

$$\Theta = \text{const.} \frac{1}{D}$$

The discussed patterns are therefore represented on the log-log plot by three arrows strongly inclined to the ordinate (fig. 1, VI, VII and VIIa).

Table 1 contains a numerical example of the transition $\Theta_1 \longleftrightarrow \Theta_2$ due to D or \bar{U} changes, computed using eq. 3 for the quartz silt and fine sand ($d_g = 2.65 \text{ g cm}^{-3}$), clear water ($d_f = 1.0 \text{ g cm}^{-3}$) and for the representative value of f (0.08) applied after Allen (1970).

Any changes of the grain size of the sediment transported by the unsteady and non-uniform unsteady currents effect naturally $\tan \zeta$ as well. If the grain size happened to increase when the mean flow velocity decreased or the reverse was true, the effects of these changes on climbing-ripple patterns would have summed up. The resulting complex

A numerical example of a transition from lower to upper plane bed or reversely ($Q_1 \leftarrow \rightarrow Q_2$) due to mean flow velocity or mean size of the bulked sediment changes (computation according to eq. 3 — see text)

Liczbowy przykład przejścia od fazy dolnego do górnego płaskiego dna lub odwrotnie ($Q_1 \leftarrow \rightarrow Q_2$) w wyniku: a) zmian średniej prędkości przepływu, b) zmian uziarnienia (obliczenia na podstawie równania 3 zamieszczonego w tekście)

Table 1

a)

| | | | | | | |
|-----------------------------------|------|------|------|------|------|------|
| D (μm) | 30 | | | | | |
| θ | 0.1 | 0.2 | 0.3 | 0.4 | 0.5 | |
| \bar{U} (cm sec ⁻¹) | 7.0 | 9.9 | 12.1 | 14.0 | 15.7 | |
| D (μm) | 100 | | | | | |
| θ | 0.05 | 0.1 | 0.2 | 0.3 | 0.4 | 0.5 |
| \bar{U} (cm sec ⁻¹) | 9.0 | 12.8 | 18.1 | 22.2 | 25.6 | 28.7 |

b)

| | | | | | | |
|-----------------------------------|------|-----|-----|-----|-----|-----|
| D (μm) | 350 | 139 | 50 | 48 | 35 | 28 |
| θ | 0.04 | 0.1 | 0.2 | 0.3 | 0.4 | 0.5 |
| \bar{U} (cm sec ⁻¹) | 15 | | | | | |

patterns (for the definition see p. 464) should be quite similar to simple ones produced by non-uniform current.

In the alternative situation (parallel changes of D and \bar{U}), the effects of D and \bar{U} on $\tan \zeta$ would usually subtract one from the other (fig. 5 — complex patterns {I + VII (VIIa)} and {III (IIIa) + VI}). In the normal currents, the D influence probably modifies only slightly the general tendency of $\tan \zeta$ due to \bar{U} changes. Good examples are fig. 2 (upper part) in that paper, fig. 7 and 14 in that of Jopling and Walker (1968) and some parts of units c, d, e, f, g, investigated by Aario (1972).

However, from the theoretical point of view, the complex patterns mentioned above, may resemble the simple patterns VI and VII (VIIa) (fig. 5), if the influence of the changes of grain size is dominant. Thus, it appears that identical patterns may result from non-uniform as well as from unsteady currents, the latter either accelerating or decaying, provided that D changes have been adequate. Such a puzzling structure, which shows the characteristic of D and $\tan \zeta$ corresponding with the

pattern VI, has been reported from an esker delta by Aario (1972, fig. 17 — unit b).

In these cases, it seems impossible to recognize the type of flow from the climbing-ripple pattern alone. The computations based on eq. 3, like the one in tab. Ia, cannot be performed, even if the transition $\theta_1 \longleftrightarrow \theta_2$ is reflected by sedimentary structures. As Bagnold has pointed out (1966), we cannot compute the mean grain size of bedload material (D in eq. 3), knowing only the bulked sediment size². Fortunately, the cases considered above are, probably, uncommon in nature. An interesting exception is that of turbidity currents.

According to Scheidegger and Potter (1965) in turbidites the type of decrease of grain size as a function of time is independent on the velocity decrease. It results from the grain size distribution of the parent bed exclusively. The authors distinguish three different types of size-decline curves: concave, uniform and convex. The latest shows the highest grain size decrease rates in the fine-grained parts of turbidite layers. It seems to be the most probable geological situation for the grain size decrease rate to exceed the velocity decrease rate and dominate the effect of the latter on $\tan \zeta$. Therefore, one could expect the more or less sinusoidal path of the ripple crest within the coset: a steepening of the angle of climb followed by a flattening, despite the grain size decrease. In an extreme case, the upward decrease of the ripple height and a continuous transition into horizontal lamination due to sedimentation in the upper plane bed stage should be present. A further decrease of the grain size and the current velocity may lead to the cohesive-type sedimentation.

An excellent example of the structure thus deduced is, in my opinion, fig. 10 of Jopling and Walker (1968), taken from the Carboniferous flysch of North Cornwall and distinguished by them as type C ripple-drift cross-lamination. All the elements are there visible: a grading upward from coarse silt to mud, the sinuous path of the angle of climb, a flattening of the ripples and their transition to the horizontal lamination. For other examples see Wood and Smith (1958, fig. 7, 10) and Walker (1963, fig. 7 and 1969, fig. 7). Fig. 7 of Kuenen (1967) looks similar, but some additional complications, discussed in the next chapter are probable. The apparent flattening of the ripples down to $H = 0$ is distinctive for that pattern as compared with pattern IV, implied by the analysis of Allen (1971 b).

The graphic representation of the complex pattern under study is a concave arrow pointing toward fines and twice crossing the θ_2 line

² By the way, it should be noted that, according to the above restriction, the method of estimating the deposition rate from climbing ripples, as proposed by Allen (1971 a, b), should be verified.

(fig. 1, pattern T_1). The two other patterns, theoretically expected in turbidites, are expressed by the arrows T_2 and T_3 , starting at the same point.

In the T_2 pattern, the rate of velocity decrease is the dominant quantity controlling $\tan \zeta$. The upper laminated level (K u e n e n, 1967) may be here confidently ascribed to the deposition in the lower plane bed stage. The pattern, though complex {I + VI}, is geometrically similar to pattern I (e.c. K u e n e n, 1967, fig. 6).

The pattern T_3 results from the transition to the cohesive bed type of the deposition at the fine grain side of the ripple stability field. That situation has not been, as far as I know, simulated experimentally yet, the resulting pattern still remains incomprehensible.

The concept of independent decrease of current velocity and grain size has been applied to turbidites earlier (W a l k e r, 1965) to explain the absence of some divisions of the Bouma sequence, as observed in many profiles.

Limited availability of transportable solids

As pointed out at the beginning, all the analyses presented are valid provided the basic condition formulated by B a g n o l d (1966) is satisfied: the transportation power of the current is utilized completely. Expressing that idea in more geological terms: we deal with a sediment-overloaded current. For this type of flow, B a g n o l d's sediment transport function can be used and the deposition rate is a derivative of the sediment transport rate with respect to both distance and time or to either of them (A l l e n, 1970).

However, it looks interesting to consider what happens if the availability of transportable solids is limited. Theoretically, the two processes should be taken into account:

1. the increase of the real value of the sediment transport rate j_r until the theoretical value for the fully loaded flow (j_t), determined by B a g n o l d's function, is reached,
2. the decrease of j_r from j_t towards 0.

The negative value of the deposition rate $M < 0$ remains naturally the essential condition of deposition, but B a g n o l d's theory seems to imply a second condition: $j_r \cong j_t$. If not, an erosion [or non-deposition in the case of fine-grained beds — see R e e s (1966)] will occur within the ripple stability field (fig. 1).

We are justified to expect a tangential decrease of the angle of climb of the ripples towards the erosion or the non-deposition plane in both cases distinguished, if, of course, the uppermost part of the deposited layer is not eroded (case 2). When the real value of the deposition rate (j_r) is very close to j_t so that $j_r > j_t - \Delta j_t$, where $\frac{\Delta j_t}{\Delta x} \cong M$, x denoting

both distance and time, or either of them, the minute changes of j_r should effect M and — consequently — $\tan \zeta$ very strongly. If the presented analysis is true, the climbing-ripple patterns including the erosional surfaces due to the flow changes ($M > 0$) or sediment supply changes ($j_r < j_t$) are geometrically quite similar. Other data must be used to distinguish them one from the other.

The phenomenon of erosion (non-deposition) due to the underloading of the flow is likely to occur in turbidites, especially of the convex-type size-decline curve. The rapid reduction of the grain size probably results sometimes in a transition to the upper plane bed stage despite velocity decreases (p. 462). Finally, however, the non clay-grade material is lacking. The flow is likely to become underloaded and an erosion or non-deposition to take place. We should therefore expect the erosion (non-deposition) plane between the top lutite, which represents wash-load, deposited from suspension in nearly motionless conditions, and climbing ripples or horizontally laminated silt overlying them. The two instances given by S o r b y (1908) and fig. 7 of K u e n e n (1967) are likely to be explained by that model. Fig. 4 of W a l k e r (1963) looks similar, though it does not represent turbidites but alluvial channel fill.

OUTLINES OF THE PROPOSED GENETIC CLASSIFICATION

The theoretical models of the climbing-ripple cross-lamination patterns, developed in the present paper, are mostly apparent consequences of the sediment transport theory of B a g n o l d (1956, 1966), employed to analyse the equation of the angle of climb of the ripples given by A l l e n (1970). The term „pattern” is used here in a somewhat different sense than that proposed by A l l e n (1973 b):

1. It denotes the internal structure, in the vertical section parallel to the flow direction, formed due to the drift of the „alive” ripples, i.e. at the $\Theta_1 - \Theta_2$ stage of flow (fig. 1). In fig. 5, summarizing the results schematically, the structures devoted to the upper or lower plane beds are marked separately from the pattern if expected as its nearest neighbour. Their absence denotes the erosion surface due to $M > 0$, or another climbing-ripple pattern.

2. A single pattern implies that the main quantity (quantities) controlling $\tan \zeta$ is (are) qualitatively stable throughout the coset (e.g. $H \rightarrow 0$, see fig. 5).

3. Simple patterns are theoretical pure end-members produced by a single factor (e.g. grain size changes, see fig. 5³). Complex patterns represent a conjunction of two or more simple patterns taken from

³ Note that the patterns V—VIII, regarded as simple for the sake of classification clarity, are in fact the complex ones (conjunctions with the pattern II).

different factor groups (e.g. the lowest pattern on Pl. I, fig. 2 may be symbolized by {I + V}).

4. There are three main quantities variable, that should be taken into account to describe a pattern: the angle of climb of the ripples (ζ), the bulked sediment size (D), and the ripple height (H).

Consequently to the p. 1, the term „sinusoidal ripple lamination”, according to the suggestion of J o p l i n g and W a l k e r (1968), is used in preference to the type S climbing-ripple cross-lamination proposed by A l l e n (1970). The definition of the sinusoidal ripple lamination is also accepted as non-arbitrary but field-experienced (lee and stoss side laminae equal in thickness, fully homogeneous grain distribution in a lamina). Fig. 5a from the experiments of K u e n e n (1967) seems to be the best material for the discussion on the genetic status of the sinusoidal ripple lamination. In my opinion, the structure, as defined by J o p l i n g and W a l k e r (1968), is a „dead ripple” one, not fully homologous with their type A and B as regarded by A l l e n (1970, 1973 b), but rather analogous to every curved lamination gradually reducing the stable bed roughness (see e.g. S h r o c k, 1948, fig. 115, 126). The strong field evidence for the opinion is that, as far as I know, nobody has observed the sinusoidal ripple lamination starting from a plane bed. It always buries some true ripples (T w e n t h o f f e l, 1932 fig. 76; M c K e e, 1938 fig. 4a, b, 1965, fig. 3c; C r o w e l l et al., 1966 fig. 13; J o p l i n g and W a l k e r, 1968 fig. 6, 7, 11; A l l e n, 1971 b fig. 9, 15; A a r i o, 1972 — many instances). If this is the case, the sinusoidal ripple lamination is to be interpreted as the lower plane bed structure. The theoretical and experimental study of A l l e n (1971 b) supports that conclusion. He has shown that a small downcurrent shifting of the ripple crests, characteristic of the sinusoidal ripple lamination, may be produced after bedload movement has ceased, the process being due to the imbalance of suspending ability between the two faces of the ripple.

Consequently to the genetic status discussed above, the sinusoidal ripple lamination is sketched in fig. 5 analogically to the horizontal lamination as the nearest neighbour of the climbing-ripple pattern. In nature, the fully gradational contacts are common, especially when the lee-side concentrations of coarser material are not apparent. In these cases, the differentiation must be somewhat arbitrary.

The proposed classification is restricted to the current-formed patterns; the structures due to wave action are left aside. Stationary ripple lamination is excluded, despite the fact that it has been reported from current deposits (A a r i o, 1972). However, as it has been pointed out by the author, the structure was formed in peculiar flow conditions, within the area of zero velocity, in front of an esker delta. Thus, the fluid motion, forming the ripples, was not of a current-type, but was rather analogous to that of intersecting oscillatory wave motion (A a r i o, 1972, p. 19). All

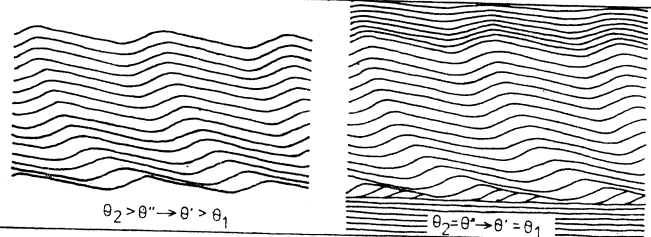
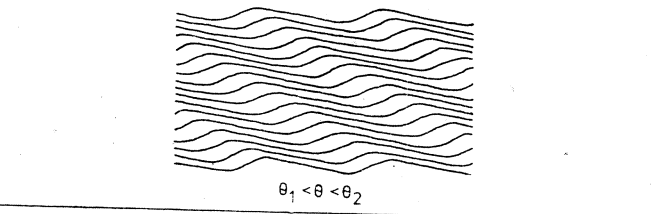
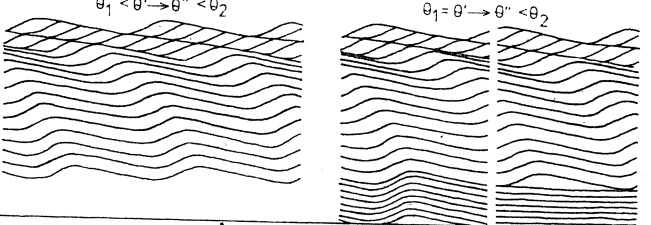
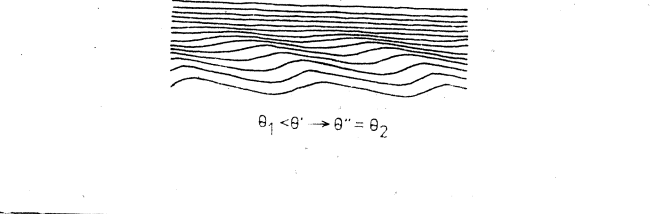
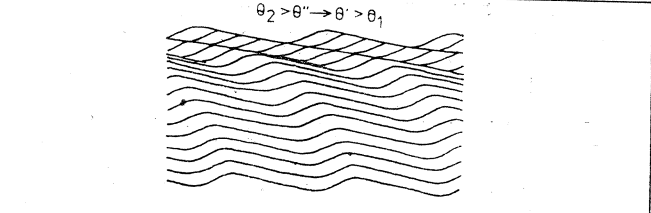
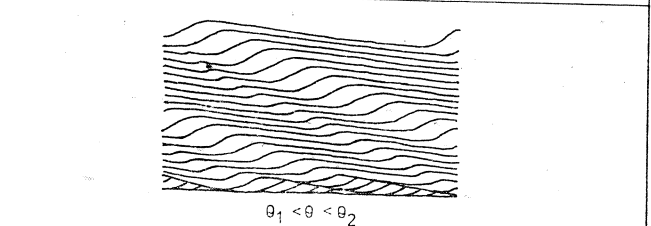
| Factor controlling $\tan \zeta$ | Number of pattern | Components of \bar{U} : | | Measurable quantities: | | | Schematic patterns | |
|---------------------------------------|---------------------|---------------------------|-------------|------------------------|--------|---|--------------------|--|
| | | non. | unst. | $\tan \zeta$ | D | H | | |
| F l u i d f l o w c h a n g e s | $j_b \rightarrow 0$ | I | — ↓ ↑ | ↓ ↓ ↓ | ↑ | C | C |  |
| | $\frac{M}{j_b} = C$ | II | ↓ | — | C | C | C |  |
| | $M \rightarrow 0$ | III | ↓ | ↑ | ↓ | C | C |  |
| | $H \rightarrow 0$ | IIIa | ↓ | ↑ | ↓ 0 | C | ↓ 0 |  |
| | $M \rightarrow 0$ | IV? | ↑ | ↓ | ↓ | C | C |  |
| Maturation | $H \rightarrow C$ | V | ↓ | — | ↑ C | C | ↑ C |  |

Fig. 5. Theoretical simple climbing-ripple patterns and their genetic interpretation. Patterns I, II, III and IV based on Allen (1970, 1971b, 1973b). The upper and lower plane bed structures marked separately (closer lines), where expected. Grain size changes marked, only when essential, close to the pattern. The upward and downward arrows denote a growth or diminishing of the corresponding quantities, respectively. J_b is the bedload transport rate, M — the deposition rate, H — the ripple height, C — constant, Q_1 — the threshold of bedload movement, Q_2 — the threshold of fully developed bedload transport, j_t — the theoretical value of the sediment transport rate, according to Bagnold equation, j_r — the real value of the sediment transport rate, \bar{U} — the mean flow velocity, non. — non-uniform, unst. — unsteady

| | Factor controlling $\tan \zeta$ | Number of pattern | Components of \bar{U} : | | Measurable quantities: | | | Schematic patterns |
|----------------------------------|---------------------------------|-------------------|---------------------------|-------|------------------------|---|-----|--------------------|
| | | | non. | unst. | $\tan \zeta$ | D | H | |
| Grain size changes | $j_b \rightarrow 0$ | VI | ↓ | — | ↑ | ↑ | C | |
| | $j_b \uparrow$ | VII | ↓ | — | ↓ | ↓ | C | |
| | $H \rightarrow 0$ | VIIa | ↓ | — | ↓ | ↓ | ↓ | |
| Limited availability of sediment | $M \rightarrow 0$ | VIIIa | ↓ | — | ↓ | 0 | C C | |
| | $M \rightarrow C$ | VIIIb | ↓ | — | ↑ | C | C C | |

Fig. 5. Teoretyczne proste wzory ripplemarków wstępujących i ich interpretacja genetyczna. Wzory: I, II, III, IV oparte na pracach Allena (1970, 1971b, 1973b) Struktury sedimentacyjne fazy górnego i dolnego płaskiego dna zaznaczone oddzielnie (gęste linie), jeżeli należy ich oczekiwać w bezpośrednim sąsiedztwie wzorów. Zmiany uziarnienia, stanowiące czynnik genetyczny, zaznaczono obok wzorów. Strzałki skierowane w górę lub w dół oznaczają odpowiednio wzrost lub zmniejszanie się danej wielkości. J_b — natężenie transportu dennego, M — natężenie depozycji, H — wysokość ripplemarku, C — wartość stała, Q_1 — próg transportu trakcyjnego, Q_2 — próg w pełni rozwiniętego transportu trakcyjnego, j_t — teoretyczna wartość natężenia transportu zgodnie z równaniem Bagnolda, j_r — rzeczywista wartość natężenia transportu, \bar{U} — średnia prędkość przepływu, non. — składowa \bar{U} , zmienna w kierunku przepływu, unst. — składowa \bar{U} , zmienna w czasie

the ripple laminations, reflecting the fluid motion of wave type, can be usually recognized on the basis of their sharp crests (see e.g. M c K e e, 1965, fig. 3c, d and A a r i o, 1972, Plate 4 and 6).

CONCLUSIONS: A SCHEME FOR DECIPHERING THE DEPOSITION
CONDITIONS FROM CLIMBING-RIPPLE CROSS-LAMINATION PATTERNS

All the simple patterns discussed in the present paper, together with those predicated by A l l e n (1971 b, 1973), are listed in fig. 5 and their genetic interpretation is provided.

The four independent major factors controlling the angle of climb of the ripples are:

1. fluid flow conditions (patterns I, II, III, IIIa, IV),
2. the maturation of the rippled bed pattern (pattern V),
3. the bulked sediment size (patterns VI, VII, VIIa),
4. a limited availability of transportable solids (pattern VIIIa, VIIIb).

To interpret climbing ripples correctly, the angle of climb, the bulked grain size, and the ripple height should be traced throughout the pattern. The nearest neighbour of the pattern should be also examined. Sometimes, some additional observations, e.g. that of the capture of ripples, are useful.

Provided the bulked sediment size is constant or varies antipathetically with the angle of climb, the pattern can usually be ascribed to flow changes. The unsteady element of flow velocity can be recognized from the angle of climb changes exclusively. Of course, the cases of the maturation of the ripple pattern and of a limited availability of transportable solids must be eliminated, when using other criteria.

The constant angle of climb usually reflects non-uniform flow conditions; however, the adequate sediment size changes in unsteady or non-uniform unsteady flow may be manifested analogically (the complex patterns {I + VII} or {III + VI}); a good example of the former is in fig. 4 of W a l k e r (1969).

If the bulked sediment size and the angle of climb changes are consistent, the type of flow (non-uniform, unsteady accelerating or decaying) is practically unrecognizable from the pattern alone. The structures of the nearest neighbour or other pieces of information are decisive in some cases (e.g. turbidity currents).

Field experience proves that the three patterns due to the flow changes, predicted by A l l e n (1970, 1971 b, 1973 b) (fig. 5, pattern I, II and III) are most common in natural environment. Other ones are considerably rarer.

Any application of the patterns proposed in the present paper for the geological interpretation of climbing ripples must be very cautious. It should be emphasized that most of them are purely theoretical models,

not simulated mathematically, the general estimates being made by simplest methods. The field, as well as experimental evidence, is now rather scarce (especially for the patterns VIIIa, b). Even provided the models are formally all right, we must remember that:

1. The critical bedload stage Θ_2 is only broadly associated with the value of Θ , at which the bed features disappear, the experimental evidence proving the correspondence to be moderate (Bagnold, 1966).

2. Bagnold theory deals with the steady open-channel flow by gravity. Its application to non-equilibrium flows is justified, but only if the flow varies gradually enough (Allen, 1970). From the viewpoint of the internal depositional structure, it means that any stage of the structure development has not been left out or radically reduced due to a rapid evolution of the hydraulic parameters of flow. If the opposite is true, the structural record of the deposition conditions cannot be complete.

3. It is possible that other factors may exist which strongly effect the climbing-ripple patterns, but are not detected yet.

The author is greatly indebted to Dr Stanisław Dżułyński and Ryszard Gradziński for discussion of the results.

Polish Academy of Sciences
Laboratory of Geology
Cracow

WYKAZ LITERATURY REFERENCES

- Aario R. (1972), Associations of bed forms and palaeocurrent patterns in an esker delta, Haapajärvi. *Ann. Acad. Sci. Fennicae*, Series A III, No. 111, 55 p. Helsinki.
- Allen J. R. L. (1968), Current Ripples. North-Holland, Amsterdam, 433 p.
- Allen J. R. L. (1970), A quantitative model of climbing ripples and their cross-laminated deposits. *Sedimentology*, 14, pp. 5—26.
- Allen J. R. L. (1971a), Instantaneous sediment deposition rates deduced from climbing-ripple cross-lamination. *J. geol. Soc. Lond.*, 127, pp. 553—561.
- Allen J. R. L. (1971b), A theoretical and experimental study of climbing-ripple cross-lamination, with a field application to the Uppsala esker. *Geogr. Ann.*, 53 A, pp. 157—187, Stockholm.
- Allen J. R. L. (1973a), Features of cross-stratified units due to random and other changes in bed forms. *Sedimentology*, 20, pp. 189—202.
- Allen J. R. L. (1973b), A classification of climbing-ripple cross-lamination. *J. geol. Soc. Lond.*, 129, pp. 537—541.
- Bagnold R. A. (1956), The flow of cohesionless grains in fluids. *Phil. Trans. R. Soc. Lond.*, A249, pp. 235—297, London.
- Bagnold R. A. (1966), An approach to the sediment transport problem from general physics. *Prof. Pap. U.S. geol. Surv.*, 422—I, 37 p.
- Ballance P. F. (1964), The sedimentology of the Waitemata Group in the Takapuna section, Auckland. *New Zealand J. Geol. Geophys.*, 7, pp. 466—499, Wellington.

- Blatt H., Middleton G., Murray R. (1972), Origin of sedimentary rocks. *Prentice-Hall, New Jersey*, 634 p.
- Boersma J. R. (1967), Remarkable types of mega cross-stratification in the fluvial sequence of a sub-recent distributary of the Rhine, Amerongen, The Netherlands. *Geol. Mijnbouw*, 46, pp. 217—235, Delft.
- Bouma A. H. (1962), Sedimentology of some Flysch Deposits. *Elsevier, Amsterdam*, 168 p.
- Coleman J. M., Gagliano S. M. (1965), Sedimentary structures: Mississippi River deltaic plain. In: G. W. Middleton (Editor), Primary Sedimentary Structures and their Hydrodynamic Interpretation — *Soc. Econ. Palaeontologists Mineralogists, Spec. Publ.*, 12, pp. 133—148. Tulsa.
- Crowell J. C., Hope R. A., Kahle J. E., Ovenshine A. T., Sans R. A. (1966), Deep water sedimentary structures of the Pliocene Pico Formation, Santa Paula Creek, Ventura Basin, California. *Calif., Dept. Nat. Resources, Div. Mines, Spec. Rept.*, 89, 40 p., San Francisco.
- Davies D. K. (1966), Sedimentary structures and subfacies of a Mississippi River point bar. *J. Geol.*, 74, pp. 234—239.
- Gilbert G. K. (1914), The transportation of debris by running water, based on experiments made with the assistance of E. C. Murphy: *U. S. Geol. Surv. Prof. Paper* 86, 263 p.
- Jopling A. V. and Walker R. G. (1968), Morphology and origin of ripple-drift cross-lamination, with examples from the Pleistocene of Massachusetts. *J. sedim. Petrol.*, 38, pp. 971—984.
- Kuennen P. H. (1967), Emplacement of flysch-type sand beds. *Sedimentology*, 9, p. 203—243.
- McBurdie E. F. (1962), Flysch and associated beds of the Martinsburg Formation, Ordovician, Central Appalachians. *J. sedim. Petrol.*, 32, pp. 39—91.
- McKee E. D. (1938), Original structures in Colorado River flood deposits of Grand Canyon. *J. sedim. Petrol.*, 8, pp. 77—83.
- McKee E. D. (1965), Experiments on ripple lamination. In: G. W. Middleton (Editor), Primary Sedimentary Structures and their Hydrodynamic Interpretation — *Soc. Econ. Paleontologists Mineralogists, Spec. Publ.*, 12, pp. 66—83, Tulsa.
- McKee E. D. (1966), Significance of climbing-ripple structure. *Prof. Pap. U. S. geol. Surv.*, 550-D, pp. 94—103.
- McKee E. D., Crosby E. J., Berryhill H. L. (1967), Flood deposits, Bijou Creek, Colorado, June 1965. *J. sedim. Petrol.*, 37, pp. 829—851.
- Picard M. D., High L. R. Jr. (1973), Sedimentary structures of ephemeral streams. *Elsevier, Amsterdam*, 223 p.
- Rees A. I. (1966), Some flume experiments with fine silt. *Sedimentology*, 6, pp. 209—240.
- Sanders J. E. (1963), Concepts of fluid mechanics provided by primary sedimentary structures. *J. sedim. Petrol.* 33, pp. 173—179.
- Scheidegger A. E., Potter P. E. (1965), Textural studies of graded bedding. Observation and theory. *Sedimentology*, 5, pp. 289—304.
- Scheidegger A. E., Potter P. E. (1967), Bed thickness and grain size: cross-bedding. *Sedimentology*, 8, pp. 39—44.
- Shrock R. R. (1948), Sequence in layered rocks. *McGraw-Hill, New York*, 507 p.
- Simons D. B., Richardson E. V., Nordin C. F. Jr. (1965), Sedimentary structures generated by flow in alluvial channels. In: G. W. Middleton (Editor), Primary Sedimentary Structures and their Hydrodynamic Interpretation. *Soc. Econ. Palaeontologists Mineralogists, Spec. Publ.*, 12, pp. 34—52, Tulsa.

- Sorby H. C. (1908), On the application of the quantitative methods to the study of the structure and history of rocks. *Quart. J. geol. Soc. Lond.*, 64, pp. 171—233.
- Southard J. B., Ashley G. M., Boothroyd J. C. (1972), Flume simulation of ripple-drift sequences. *Abstracts with Programs* 4, p. 672.
- Southard J. B., Boguchwal L. A. (1972), Transition from ripples to lower flat bed with increasing grain size in open-channel flow. *Abstracts with Programs* 4, pp. 672—673.
- Środoń J., Montmorillonitic claystones with climbing-ripple cross-lamination from the Upper Silesian Coal Basin, Poland (in preparation).
- Twenthoffel W. H. (Editor) (1932), Treatise on Sedimentation. *Williams and Wilkins*, Baltimore, 926 p.
- Walker R. G. (1963), Distinctive types of ripple-drift cross-lamination. *Sedimentology*, 2, pp. 173—188.
- Walker R. G. (1965), The origin and significance of the internal sedimentary structures of turbidites. *Proc. Yorkshire geol. Soc.*, 33, pp. 1—29, Hull.
- Walker R. G. (1969), Geometrical analysis of ripple-drift cross-lamination. *Can. J. Earth. Sci.*, 6, pp. 383—391.
- Wood A., Smith A. J. (1959), The sedimentation and sedimentary history of the Aberystwyth Grits (Upper Llandoveryan). *Quart. J. geol. Soc. Lond.*, 114, pp. 163—195.

STRESZCZENIE

Zgodnie z badaniami autora jednoznaczny opis warstwy ripplemarków wstępujących w danym przekroju pionowym, równoległym do kierunku prądu wymaga podania zmienności pionowej trzech wielkości: kąta wspinania się ripplemarków, uziarnienia oraz wysokości ripplemarków. Uwzględnienie tej trzeciej wielkości narzuca konieczność uzupełnienia opisowej definicji „wzoru ripplemarków wstępujących” (climbing-ripple pattern) podanej przez Allena (1973 b). Z badań tego autora (Allen, 1970, 1971 b) wynika, że najczęściej czynnikiem kontrolującym wzory ripplemarków wstępujących są zmiany przepływu w przestrzeni, czasie lub w przestrzeni i czasie równocześnie. Okazuje się jednak, że w pewnych sytuacjach decydujący wpływ na wzór ripplemarków wstępujących mają inne czynniki:

- 1) dojrzewanie wzoru ripplemarków na dnie, wyrażające się wzrostem wysokości i długości ripplemarków oraz redukcją ich pierwotnej ilości,

- 2) zmiany uziarnienia niezależne od zmian średniej prędkości przepływu,

- 3) ograniczenie podaży transportowanego materiału.

Przeprowadzone rozróżnienia umożliwiają skonstruowanie genetycznej klasyfikacji ripplemarków wstępujących (fig. 5). Podstawą jej są tzw. „proste wzory” (simple patterns), czyli teoretyczne struktury będące rezultatem działalności tylko jednego czynnika genetycznego. Należy podkreślić, że efektem wpływu jednego czynnika (np. zmian przepływu) może być kilka prostych wzorów, które należy traktować jako alternatywy.

Jako wzór złożony (complex pattern) określono koniunkcję dwu lub więcej wzorów prostych, czyli strukturę powstającą w wyniku równoczesnego działania kilku czynników genetycznych.

Niektóre z przedstawionych teoretycznych wzorów prostych i złożonych zostały zilustrowane w oparciu o materiały własne autora oraz dane z literatury.

Wygodnym sposobem symbolicznego zapisu wzorów ripplemarków wstępujących jest przedstawienie ich w postaci punktów lub strzałek w obrębie pola trwałości ripplemarków (fig. 1), skonstruowanego w oparciu o pracę Bagnolda (1966) i zmodyfikowanego oraz uzupełnionego w zakresie frakcji pyłowej zgodnie z wynikami eksperymentów Reesa (1966).

Nazwa „falista laminacja ripplemarkowa” stosowana jest w pracy zgodnie ze starszą z dwóch znanych definicji (Jopling i Walker, 1968; Allen, 1973 b). Wydaje się, że tak rozumianą strukturę przypisać należy sedymentacji z zawiesiny w fazie dolnego płaskiego dna, czyli po zaniknięciu transportu trakcyjnego.

Wzory ripplemarków wstępujących zaproponowane przez autora są w zasadzie wynikiem rozważań teoretycznych, opartych o teorię transportu Bagnolda i nie potwierdzonych eksperymentalnie. Nawet jeżeli są one poprawne, zasadnicze ograniczenie ich stosowania wynika z ograniczonej stosowalności teorii Bagnolda (sformułowanej dla warunków ustalonego przepływu) do przepływów naturalnych.

*Pracownia Sedymentologii
ZNG PAN,
31—002 Kraków, Senacka 3*

OBJAŚNIENIE TABLIC EXPLANATION OF PLATES

Plate — Tablica I

- Fig. 1. The sinuous ripples corresponding to the climbing-ripple patterns shown on Pl. I. fig. 2. The negatives of the ripples are visible, as exposed on the roof of a gallery. The example taken from Carboniferous montmorillonitic claystones of the Upper Silesian Coal Basin.
- Fig. 1. Strop wyrobiska z zachowanymi negatywami ripplemarków krętych, odpowiadających ripplemarkom wstępującym przedstawionym na tabl. II, fig. 2. Przykład pochodzi z karbońskich ilowców montmorillonitowych z Górnośląskiego Zagłębia Węglowego.
- Fig. 2. A complex pattern. {I + V} covered by sinusoidal ripple lamination and pattern III. In the bottom part of the complex pattern the ripple height increase as well as the capture of ripples, both characteristic of the maturation process, can be traced.
- Fig. 2. Złożony wzór ripplemarków wstępujących {I + V} przykryty przez falistą laminację ripplemarkową i wzór III. W dolnej części wzoru złożonego wi-

doczny jest wzrost wysokości ripplemarków oraz zmniejszanie się ich ilości. Obydwa te zjawiska są charakterystyczne dla procesu dojrzewania powierzchni ripplemarkowej.

Plate — Tablica II

Fig. 3. The coset of climbing ripples deposited from the non-uniform current (pattern II), with two layers disturbed by convolute deformation and having the top planes smoothed out by liquefaction. The tangential growth of the angle of climb of ripples just above the liquefaction plane, due to a maturation of the rebuilt ripple pattern (pattern V). Carboniferous montmorillonitic claystones of the Upper Silesian Coal Basin.

Fig. 3. Fragment warstwy ripplemarków wstępujących, zdeponowanej przez prąd o średniej prędkości zmniejszającej się w kierunku przepływu, ale stałej w czasie (wzór II). Widoczne dwie warstwy zaburzone przez deformacje konwolutive, o płaskich powierzchniach stropowych związanych z upłynnieniem. Stopniowy wzrost kąta wspinania się ripplemarków nad powierzchnią upłynnienia (wzór V) jest wynikiem dojrzewania powierzchni ripplemarkowej. Karbońskie iłowce montmorillonitowe z GZW.

Fig. 4. Pattern V — a detail from Pl. II, fig. 3. The lee-side concentrations of coal detritus visible. A match in the upper right.

Fig. 4. Powiększony fragment wzoru V z tabl. II, fig. 3. Widoczna koncentracja detrytus węgłowego na stokach zaprądowych ripplemarków. Zapałka w prawym górnym rogu.



